

This is an Open Access document downloaded from ORCA, Cardiff University's institutional repository: <https://orca.cardiff.ac.uk/id/eprint/111718/>

This is the author's version of a work that was submitted to / accepted for publication.

Citation for final published version:

Schwarz, Martin, Garnica, Manuela, Fasano, Francesco, Demitri, Nicola, Bonifazi, Davide and Auwärter, Willi 2018. BN-patterning of metallic substrates through metal coordination of decoupled borazines. *Chemistry - A European Journal* 24 (38) , pp. 9565-9571. 10.1002/chem.201800849

Publishers page: <http://dx.doi.org/10.1002/chem.201800849>

Please note:

Changes made as a result of publishing processes such as copy-editing, formatting and page numbers may not be reflected in this version. For the definitive version of this publication, please refer to the published source. You are advised to consult the publisher's version if you wish to cite this paper.

This version is being made available in accordance with publisher policies. See <http://orca.cf.ac.uk/policies.html> for usage policies. Copyright and moral rights for publications made available in ORCA are retained by the copyright holders.



# BN-Patterning of Metallic Substrates through Metal Coordination of Decoupled Borazines

Martin Schwarz,<sup>+[a]</sup> Manuela Garnica,<sup>+[a]</sup> Francesco Fasano,<sup>+[b]</sup> Nicola Demitri,<sup>[c]</sup> Davide Bonifazi,<sup>\*[b]</sup> and Willi Auwärter<sup>\*[a]</sup>

**Abstract:** We report on the synthesis of pyridine-terminated borazine derivatives, their molecular self-assembly as well as the electronic properties investigated on silver and copper surfaces by means of scanning tunneling microscopy and X-ray photoelectron spectroscopy. The introduction of pyridine functionalities allows us to achieve distinct supramolecular architectures with control of the interdigitation of the molecules by surface templating. On silver surfaces, the borazine derivatives arrange in a dense-packed hexagonal structure through van der Waals and H-bonding interactions, whereas on Cu(111), the molecules undergo metal coordination. The porosity and coordination symmetry of the reticulated structure depends on the stoichiometric ratio between copper adatoms and the borazine ligands, permitting an unusual three-fold coordinated Cu-pyridyl network. Finally, spectroscopy measurements provide evidence that the borazine core is electronically decoupled from the metallic substrate. We thus integrate for the first time BNC-containing molecular units into stable, metal-coordination architectures on surfaces, opening pathways to patterned, BN-doped sheets with specific functionalities, e.g., regarding the adsorption of polar guest gases.

## Introduction

Borazine derivatives have recently attracted increasing interest as molecular building blocks,<sup>[1,2]</sup> due to their high potential for applications in the fields of electronics,<sup>[3,4-6]</sup> and non-linear optics.<sup>[7]</sup> In particular hybrid *h*-BNC nanostructures, where carbon-carbon bonds are replaced by isoelectronic and isostructural BN couples are emerging as a new route to functionalize polycyclic aromatic hydrocarbons without a significant structural perturbation of the molecular periphery and of its skeleton.<sup>[6,8]</sup> The presence of BN bonds imparts strong local dipole moments that can tailor both, the optoelectronic properties and the self-assembly behavior of the molecule.<sup>[9,10]</sup> For instance, one can conjecture that the polar BN bonds could serve as anchoring point for non-covalent adsorption of polar gases like CO<sub>2</sub> and CO, which can in principle interact with BN bonds through dipolar interactions, thus making BN-doped materials very good candidates for gas adsorption.<sup>[11]</sup> Together with the

possibility of tuning the molecular band gap into the visible range of the solar spectrum, these structures could emerge as unique photoactive materials triggering photochemical transformations. Given these premises, we conjectured that two-dimensional structures formed through non-covalent interaction on a surface could act as unique model architectures to study the self-assembly and recognition properties of BN-materials at the molecular level through scanning probe microscopy (STM).

In particular, precisely tailored substituents of molecules can be utilized to realize targeted adsorption geometries, as well as to preserve the intrinsic properties of molecules upon adsorption on a metal support.<sup>[12]</sup> Recently, it has been proposed that a BN core of a molecule can be protected and electronically decoupled from the conductive substrate by di-methylphenyl terminal groups through steric hindrance without affecting the possibility of the molecule itself to adsorb and self-assemble.<sup>[13]</sup> Additionally, the selection of the substituent's termination (e.g. –carbonitrile (CN), –carboxylate, –pyridyl) steer the supramolecular interactions, driving for example the formation of two dimensional metal-organic coordination networks (2D-MOCNs) in the presence of metal adatoms. The formation of such a 2D-MOCN combining borazine and metal adatoms has not been reported to date, although those porous architectures are highly appealing as they can act as templates featuring cavities and molecular units on regular and well-defined sites linked by metallic nodes.<sup>[14]</sup> Indulging this line of thought, here we describe the synthesis and the self-assembly properties of borazine derivatives on Cu(111), Ag(100) and Ag(111) surfaces that, exposing peripheral pyridyl (py) groups, can undergo metal-coordination in the presence of additional copper adatoms to yield porous patterns. Specifically, STM studies show that the molecules behave differently on the two metal substrates, with those deposited on Ag undergoing self-assembly through van der Waals (vdW) and H-bonding interactions, whereas on Cu the molecules interact through metal-coordination. Using scanning tunneling spectroscopy (STS), we also provide evidence supporting the idea that the borazine core is electronically decoupled from the conductive metal substrate. The architectures on Cu(111) substrates were exposed to CO gas and their chemical properties investigated by XPS. Additionally, we explore the thermal stability of the network on Cu(111) at room temperature, and the effect of post-annealing on both metal substrates by STM.

## Synthesis of BNPPy and BNAPy

The pyridine-bearing borazines have been prepared following the BCl<sub>3</sub> condensation protocol (see SI for synthesis procedure).<sup>[4,5]</sup> Starting from aniline, which was reacted with BCl<sub>3</sub> under refluxing conditions, B<sub>3</sub>B<sup>+</sup>·B<sup>-</sup>-trichloro-N,N',N''-triphenyl borazine intermediate was obtained. Subsequent treatment with *tert*-butyldimethylsilyl (TBDMS)-aryllithium (ArLi) **1**, TBDMS protected borazine **2** could be prepared in 78% yield (Scheme 1). Removal of the TBDMS protecting group with TBAF and successive

[a] Martin Schwarz,<sup>\*</sup> Dr. Manuela Garnica,<sup>\*</sup> Prof. Dr. Willi Auwärter  
Department of Physics, Technical University of Munich, 85748  
Garching, Germany, Email: wau@tum.de

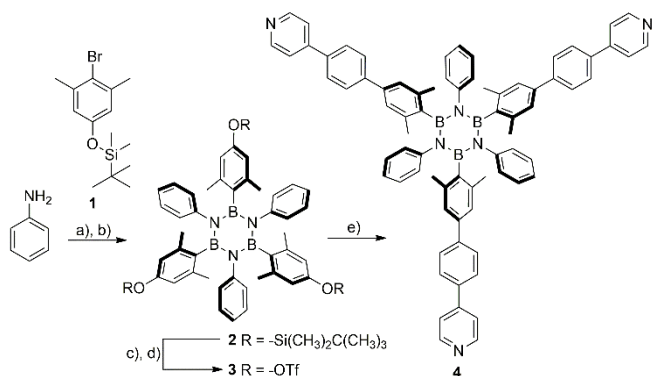
[b] Francesco Fasano,<sup>\*</sup> Prof. Dr. Davide Bonifazi  
School of Chemistry, Cardiff University, Park Place Main Building,  
Cardiff CF10 3AT, United Kingdom, Email: bonifazid@cardiff.ac.uk

[c] Dr. Nicola Demitri  
Elettra – Sincrotrone Trieste, S.S. 14 Km 163.5 in Area Science  
Park, 34149 Basovizza – Trieste, Italy

[+] These authors contributed equally.

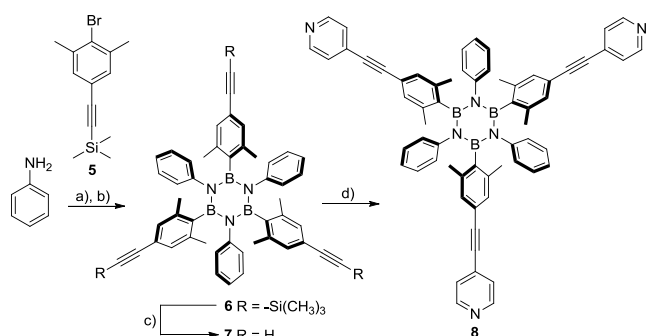
Supporting information for this article is given via a link at the end of the document.

esterification with  $\text{Tf}_2\text{O}$  in pyridine, gave tri-triflate borazine **3** in 78% yield. Final Suzuki cross-coupling reaction between molecule **3** and pyridylphenylboronic acid, led to the formation of borazine **4** (**BNPPy**) in 87% yield. Crystals suitable for X-ray diffraction analysis were obtained by slow diffusion of pentane in a  $\text{CHCl}_3$  solution of **1** (Figure 1a). The crystal packing shows hydrophobic contacts between neighbor molecules, with partial  $\pi \cdots \pi$  stacking involving the aryl arms. The effective packing of **BNPPy** in the solid phase gives rise to distorted planar arrangement of the molecules, piled up along crystallographic  $c$  axis and with partial overlaps of outer pyridine moieties of neighbor molecules (the angle between neighboring borazine ring planes is  $53^\circ$ ).



**Scheme 1.** Synthesis of **BNPPy 4**: a)  $\text{BCl}_3$ , toluene, reflux, 18 h; b) **1**,  $t\text{BuLi}$ , THF,  $-84^\circ\text{C}$ , 2 h, 78%; c) TBAF, THF,  $0^\circ\text{C}$ , 2 h; d)  $\text{Tf}_2\text{O}$ , pyridine, r.t., 16 h, 78%; e) 4-pyridinylphenylboronic acid,  $[\text{Pd}(\text{PPh}_3)_4]$ ,  $\text{K}_2\text{CO}_3$ , dioxane/ $\text{H}_2\text{O}$  (3:1),  $105^\circ\text{C}$ , 18 h, 87%.

Similarly, when  $\text{B}_2\text{B}''\text{-trichloro-N,N',N''}$ triphenyl borazine intermediate was reacted with trimethylsilyl (TMS)-protected ArLi derivative **5**, TMS-protected borazine derivative **6** could be prepared in 71% (Scheme 2). Removal of the silyl protecting group with TBAF yielded phenylacetylenborazine derivative **7**, that could be transformed into borazine **8** (**BNAPy**) by Sonogashira cross coupling reaction with 4-iodo-aniline affording.



**Scheme 2.** Synthesis of **BNAPy 8**: a)  $\text{BCl}_3$ , toluene, reflux, 18 h; b) **5**,  $t\text{BuLi}$ , THF,  $-84^\circ\text{C}$ , 16 h, 71%; c) TBAF, THF,  $0^\circ\text{C}$ , 2 h, 94%; d) 4-iodo-pyridine,  $[\text{PdCl}_2(\text{PPh}_3)_2]$ ,  $\text{PPh}_3$ ,  $\text{CuI}$ ,  $\text{NEt}_3$ ,  $75^\circ\text{C}$ , 17 h, 70%.

## Results

High-resolution STM images of individual **BNPPy** molecules on  $\text{Cu}(111)$  and  $\text{Ag}(100)$  display sub-molecular features with a very similar appearance (Figure 1b and c). The central part of the molecule appears as three bright lobes pointing along the axes

defined by the pyridyl-terminated substituents, which are imaged dimmer. The molecular contrast does not change for moderate bias voltages of both polarities, suggesting that it reflects the molecular conformation. Simulated STM images based on the extended Hückel method (see SI, Figure S25) of different adsorption geometries indicate that the **BNPPy** molecule deforms upon surface adsorption. The best agreement between experiment and simulation is obtained for a geometry where the borazine core and the peripheral pyridyl-groups are aligned (nearly) parallel to the surface plane while all phenyl rings are rotated out of this plane. Specifically, the three prominent lobes observed in STM can be reasonably associated with the bulky dimethyl-bearing aryl rings. This assignment is in line with STM observations and complementary molecular dynamics (MD) modeling reported for dimethyl-bearing aryl borazine derivatives on  $\text{Au}(111)$  and  $\text{Cu}(111)$ .<sup>[13]</sup> Consistently, we observe a very similar intramolecular contrast featuring three bright protrusions for **BNAPy** on  $\text{Cu}(111)$  (see Figure 4).

The crystal structure determined by X-ray diffraction shows that the expected three-fold symmetry from the molecule structure can be disturbed due to the flexibility of the substituents (Figure 1a). Upon adsorption, a similar behavior is observed, as can be seen in Figures 1b and c. The py-terminated substituents do not appear straight and the angles enclosed by them deviate from  $120^\circ$ .

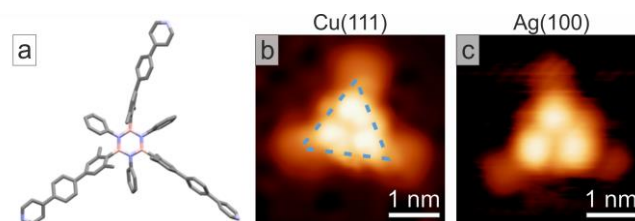


**Figure 1.** (a) Crystal structure of **BNPPy** determined by X-ray diffraction. STM images of an individual **BNPPy** molecule on (b)  $\text{Cu}(111)$  ( $U_b = 1.9\text{ V}$ ,  $I_t = 170\text{ pA}$ ) and (c)  $\text{Ag}(100)$  ( $U_b = 0.5\text{ V}$ ,  $I_t = 81\text{ pA}$ ). The superimposed dashed triangle in (b) indicates the orientation of the molecule.

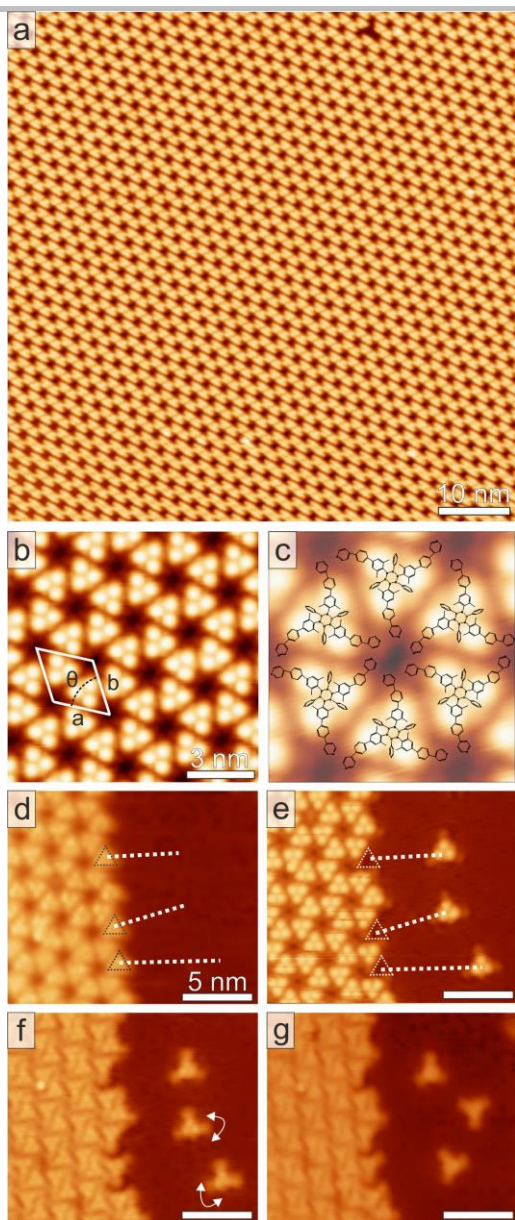
## The borazine derivative **BNPPy** on $\text{Ag}$ surfaces

Extended, highly ordered molecular islands of **BNPPy** were observed on silver samples with different surface terminations, namely a  $\text{Ag}(100)$  single crystal and a  $\text{Ag}(111)$  film (see Figures 2 and 5c, respectively). The molecules, deposited onto the sample held at room temperature, arrange in six-membered rings and form porous honeycomb networks. A similar self-assembly was observed for related molecules on the  $\text{Au}(111)$  surface.<sup>[13]</sup> Network domains with sizes of several hundreds of nm and arbitrary orientation with respect to the crystal high-symmetry directions were present on the samples.

A high-resolution close-up view (Figure 2b) reveals that each molecule in the honeycomb structure is surrounded by three neighbors and three pores. The rhombic unit cell (white lines in Figure 2b) has the parameters  $a = b = (26.0 \pm 0.5)\text{ \AA}$  and  $\theta = (60 \pm 3)^\circ$ , which results in a packing density of  $0.34\text{ molecules/nm}^2$ . The network is stabilized by intermolecular vdW and H-bonding interactions between the aryl moieties decorating the BN core. The close molecule-molecule distance suggests that the flexible substituents are presumably bent to reduce steric hindrance (see Figure 2c).

**Figure 2.** STM images of **BNPPy** on  $\text{Ag}(100)$ . (a) Large-scale image of the close-packed hexagonal network of **BNPPy** molecules. Scan parameters:





$U_b = 1.0$  V,  $I_t = 64$  pA. (b) High-resolution STM image where the unit cell is highlighted. Scan parameters:  $U_b = 0.2$  V,  $I_t = 40$  pA (c) STM image overlaid with a tentative structural model of the molecule. (d) Individual molecules can be manipulated *via* STM in a controlled way (dotted white lines). (e) Three individual **BNPPy** molecules were detached from the dense-packed island. (Scan parameters of (d) and (e):  $U_b = 0.5$  V,  $I_t = 81$  pA) (f), (g) Additionally, the orientation of the protruding substituents can be changed as indicated by the white arrows in (f). Scan parameters of (f) and (g):  $U_b = 1.7$  V,  $I_t = 81$  pA.

Nevertheless, STM-based manipulation experiments indicate weak intermolecular attraction as individual molecules can be removed from the edges of the islands in a controlled fashion without significantly perturbing the self-assembled network (Figure 2d,e). For this purpose, the STM tip is positioned above a rim molecule, which is dragged out to the bare Ag terrace (indicated by the white dashed lines) applying a bias voltage  $U_b = 50$  mV and a tunneling current  $I_t = 20$  nA. Furthermore, the molecules can be rotated by STM manipulation, changing the orientation of the pyridyl-terminated substituents with respect to the molecular axes (Figure 2f,g). The flexibility of the substituents is clearly revealed in Figure 2f where apparent angles between

$120^\circ$  and almost  $180^\circ$  are observed between adjacent aryl substituents.

In addition to the most abundant arrangement in six-membered rings, a second densely packed phase (packing density  $0.41$  molecules/nm<sup>2</sup>) embedded in the honeycomb network is occasionally observed (see SI, Figure S26). In this phase, **BNPPy** are assembled in rows consisting of pairs of molecules oriented in opposite directions. This pair of molecules constitutes the base unit observed in both structures on the Ag substrates, suggesting that the molecular packing is governed by the same intramolecular interactions and the concentration of molecules on the surface (see Figure 2 and S27). Large coverage deposition promotes the formation of the second phase, which presents a more compact network.

After annealing the sample to 570 K, the hexagonal arrays are still observed, including some dislocation lines. Additionally, disordered regions are observed (Figure S27b) where covalent structures, formed through thermal activation of C-H bonds, are presumably present.

### The borazine derivative **BNPPy** on Cu(111)

The self-assembly behavior of **BNPPy** molecules on Cu(111) is summarized in Figure 3a. A highly ordered porous 2D network with molecules arranged in interconnected chains (Figure 3d) is formed for molecules deposited onto the sample at room temperature. The trapezoidal unit cell of the network has the parameters  $a = (38.4 \pm 2.9)$  Å,  $b = (26.5 \pm 2.3)$  Å and  $\theta = (75 \pm 5)^\circ$ . The packing density is  $0.20$  molecules/nm<sup>2</sup> and the short axis of the unit cell is found to be parallel to one of the  $\langle 1\bar{1}0 \rangle$  directions of the Cu(111) surface. The growth of the network initiates at step edges where the molecules adsorb preferentially at low coverage. Subsequently, the anisotropic islands develop onto the terraces from those step edges (see SI, Figure S28a). A similar self-assembled chain-like structure was observed for the borazine derivative **BNAPy** on the same surface (see Figure 4). Due to the reduced length of the aryl substituents they present a smaller trapezoidal unit cell with the parameters  $a = (32.6 \pm 2.6)$  Å,  $b = (19.2 \pm 2.4)$  Å and  $\theta = (75 \pm 4)^\circ$ .

Along the rows, the molecules are alternately rotated by  $(60 \pm 6)^\circ$  and remarkably close-packed. The center-to-center distance is  $(20.5 \pm 0.5)$  Å for **BNPPy** and  $(17.9 \pm 0.4)$  Å for **BNAPy**, suggesting that the substituents are slightly bent. Adjacent rows are connected *via* opposing substituents in **BNPPy** and **BNAPy** networks with a center-to-center distance of  $(32.2 \pm 0.6)$  Å and  $(27.2 \pm 0.5)$  Å, respectively. This long distance suggests a pyridyl-Cu-pyridyl coordination motif, where the N atoms of the peripheral pyridyl groups are coordinated to a copper atom. Notably, due to the flexibility of the lateral aryl substituents, the molecules are not necessarily connected in a straight line. This results in the formation of a porous network featuring voids of unequal size (Figure S29).<sup>[15]</sup>

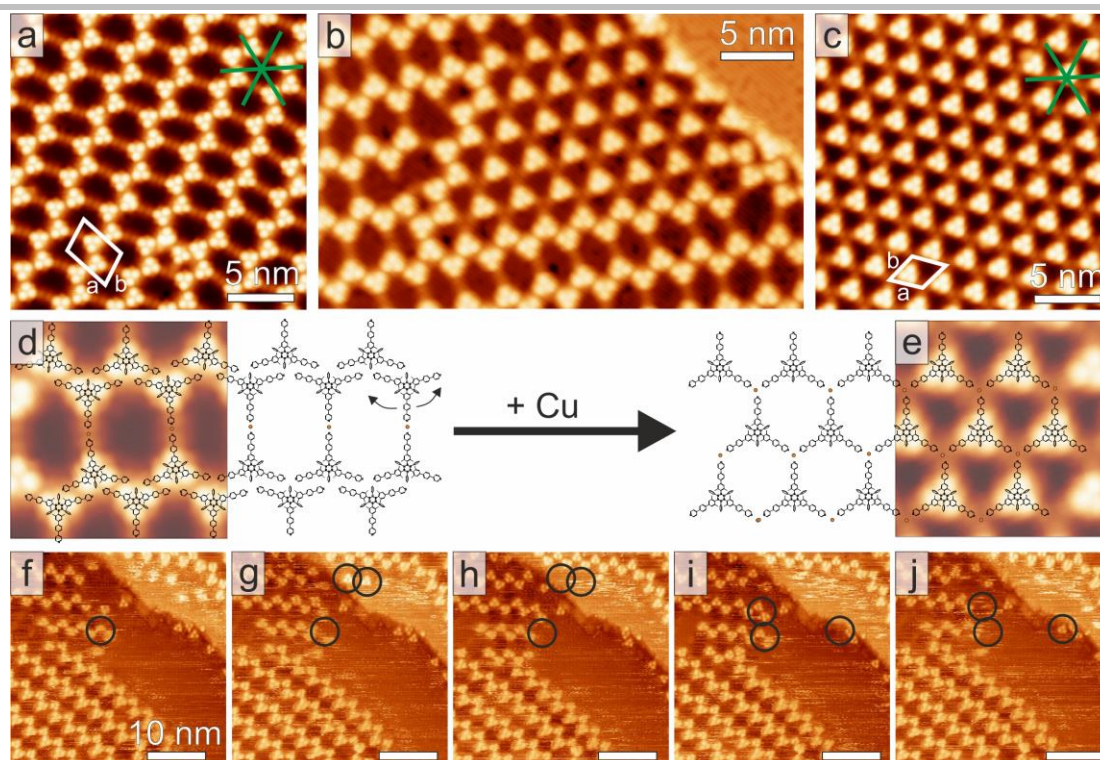


**Figure 3:** STM images displaying the self-assembly of **BNPPy** on Cu(111). (a) In the self-assembled nanostructure, the **BNPPy** molecules form rows that are interconnected by the protruding substituents coordinated to a Cu atom. Scan parameters:  $U_b = 1.2$  V,  $I_t = 100$  pA. (b) Deposition of additional Cu atoms while the sample is held at 420 K, leads to a structural transformation and patches of molecules with all three substituents coordinated to Cu atoms are formed. Scan parameters:  $U_b = 1.0$  V,  $I_t = 64$  pA. (c) With a sufficient number of available Cu adatoms, extended islands with fully three-fold coordinated **BNPPy** molecules are observed. Scan parameters:  $U_b = 0.96$  V,  $I_t = 40$  pA. (d),(e) Tentative structural models of the chain-like network and the fully reticulated network superimposed on STM images. (f)-(j) A series of STM images acquired at 300 K reveals that the metal-organic network is still observed at room temperature. Individual molecules at the edge of the molecular islands are mobile as can be seen in consecutive scans of the same region. Scan parameters:  $U_b = 1.0$  V,  $I_t = 110$  pA.

Deposition of additional copper atoms with the sample kept at 420 K gives rise to a structural transformation of the chain-like network: patches of fully Cu-coordinated hexagonal arrays embedded in the former assembly of **BNPPy** on Cu(111) emerge (Figure 3b). Annealing to this temperature in the absence of extra copper atoms or deposition of the molecules at 420 K is not sufficient to trigger the formation of the new phase. In this new network, three **BNPPy** molecules are coordinated with the N atoms of their terminal pyridyl groups to a node that presumably consists of a single Cu atom (see discussion below). As in the previous chain-like assembly, the individual Cu atoms are not resolved in the STM images. Increasing the dose of additional Cu atoms transforms the self-assembled architecture into a three-fold coordinated, fully reticulated metal-organic framework (Figure 3c,e and Figure S28b). The trapezoidal unit cell has the parameters  $a = (25.5 \pm 1.7)$  Å,  $b = (24.2 \pm 1.6)$  Å with an internal angle  $\theta = (60 \pm 2)^\circ$ , resulting in a packing density of 0.18 molecules/nm<sup>2</sup>. Notably, the nanostructure does not align with the high symmetry directions of the crystal surface.

Further annealing of either network to temperatures higher than 470 K results in a polymeric phase. Contrary to a recent study employing bromine-substituted borazine derivatives aiming for highly regular polymeric nanostructures,<sup>[16]</sup> only disordered structures were observed. Molecules have presumably lost part of their peripheral substituents and are bond covalently (see SI, Figure S27a). A similar observation was made for the dense packed structure on the Ag substrate, when it was annealed to 570 K (see SI, Figure S27b).

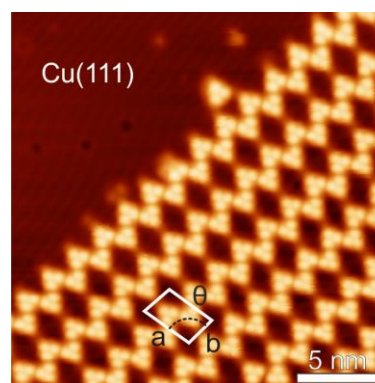


**Figure 4:** STM image of **BNPPy** on Cu(111) showing the self-assembly in molecular chains, connected through Cu-coordinated substituents. The trapezoidal unit cell has the parameters  $a = (32.6 \pm 2.6)$  Å,  $b = (19.2 \pm 2.4)$  Å and  $\theta = (75 \pm 4)^\circ$ . Scan parameters:  $U_b = 1.0$  V,  $I_t = 100$  pA.

STM measurements conducted at 300 K (Figure 3f-j) reveal that the **BNPPy** molecule form the same network as that observed on Cu(111) at low-temperature (Figure 3a). However, subsequent scans of the edge region of a molecular island suggest that the borazine modules are mobile, while the bulk of the self-assembled architecture remains mostly unperturbed. Likely, this is a consequence of the weak molecule-substrate interaction combined with the high mobility of the Cu adatoms at room temperature that, enabling the diffusion of the molecules, allow



the dynamic formation of new coordination bonds at the periphery of the self-assembled islands.

Finally, we have carried out XPS measurements on the metal-coordinated network on Cu(111) in order to investigate the ability of the **BNPPy** molecule to adsorb CO through its central borazine core – thus exploring the potential binding of polar guest gases alluded to in the introduction. XP core-level spectra of a sub-monolayer of **BNPPy** on Cu(111) before dosing CO are shown in Figure S30. The C 1s core level is observed at a binding energy  $E_b = 284.8$  eV. The N 1s core level is found at a binding energy  $E_b = 399.2$  eV. Due to its low cross-section, the B 1s core-level could not be resolved for sub-monolayer coverage. In **BNPPy** multilayers on Cu(111), the C 1s and N 1s core levels (see SI, Figure S31) reveal a slight upshift by 0.4 eV and 0.2 eV, respectively. This is attributed to a suppressed polarization screening by the metallic substrate in case of the multilayer.

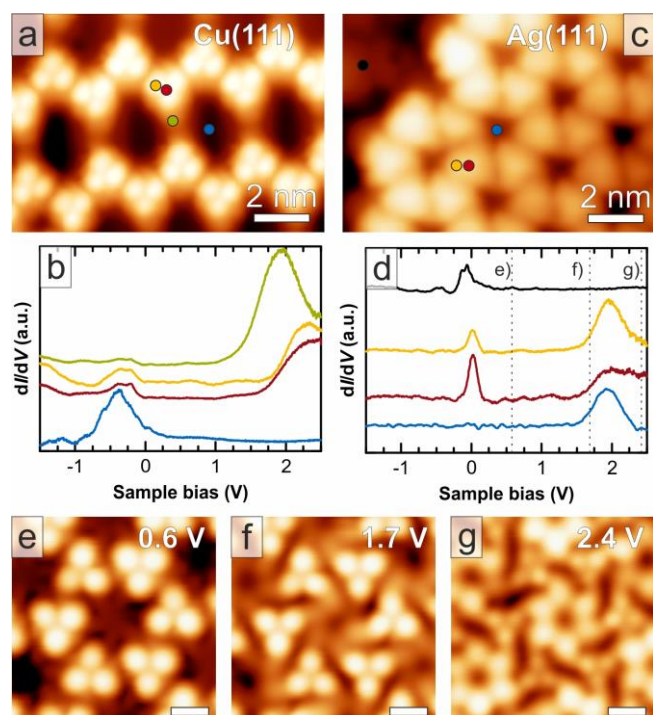


**Figure 5.** STM images of **BNPPy** on (a) Cu(111) and (c) Ag(111) (Scan parameters in both images:  $U_b = 1.0$  V,  $I_t = 100$  pA). The corresponding STS spectra recorded on characteristic positions of the respective assembly are shown in (b) and (d). (e)-(g) Voltage series of **BNPPy** on Ag(111). The scale bar is 1 nm. Set point:  $I_t = 200$  pA.

After a CO dosage of 60 L at room temperature and a dose of 6 L at  $\sim 100$  K, no noticeable changes in either core level have been observed in XPS for sub-monolayer coverages. Also in STM measurements no structural changes were detected after an *in-situ* dose of 10 L of CO at temperatures below 15 K. Therefore, we infer that the CO is not adsorbed on the self-assembled network. Presumably, this is caused by the presence of the sterically-hindering methyl substituents that, shielding the  $B_3N_3$  core, impede the formation of favorable dipolar interactions between the BN bonds and CO gas molecules.

## Spectroscopic characterization of **BNPPy**

Scanning tunneling spectroscopy (STS) data of **BNPPy** on a Cu(111) single crystal and Ag(111) film are summarized in Figure 5. In the case of Cu(111), the spectra taken in the pore of the chain-like assembly (Figure 5b, blue spectrum) show a pronounced feature at  $\sim -400$  mV, which is attributed to the increase of the local density of states due to the surface state of the Cu(111) surface. This feature is still detected in the spectra taken at the center (red spectrum) and at the bright lobe (yellow spectrum) of the molecule as indicated in Figure 5a. In analogy to reports in the literature for other physisorbed adsorbates,<sup>[17]</sup> the persistence of the surface state feature signals that the borazine core is only weakly interacting with the substrate. Moreover, an additional broad resonance is observed at 2.3 V, reflecting an electronic feature of the **BNPPy** molecule, as no such signature is observed on the bare metal. Spectra taken at the coordinated pyridyl substituent (Figure 5b, green spectrum) show a pronounced resonance shifted by  $\sim 350$  mV toward lower energy compared to the spectral feature observed on the molecular core. Indeed, the alignment and spatial distribution of molecular orbitals can be affected by the site-specific bonding with metal adatoms as previously reported.<sup>[18,19]</sup>

In the case of **BNPPy** on the Ag(111) film, the lowest unoccupied molecular resonance is found at  $\sim 2$  eV and the related surface state feature at  $\sim -50$  meV (Figure 5d, black spectrum) is also detected on the core of the molecule (red and yellow spectrum). However, for spectra taken at the center of the pore (Figure 5c, blue dot), the surface state feature is not observed. This can be tentatively explained by the presence of the terminal pyridyl rings (see Figure 2c), which are clearly visualized in STM images only at certain bias voltage. They interact with the surface and the real pore size is drastically reduced compared to that appearing at low bias voltages. Indeed, this bias dependent contrast is revealed in an STM voltage series of **BNPPy** on Ag(111) displayed in Figures 5e-g. At low bias voltages, the contrast of the **BNPPy** molecule is dominated by the three bright protrusions in the center, while the peripheral substituents are only faintly visible (Figure 5e,  $U_b = 0.6$  V). At higher bias voltages, the terminal pyridyl groups of the substituents are imaged brighter than the molecular core (Figure 5g,  $U_b = 2.4$  V), indicative of localized unoccupied molecular resonances shifted toward lower energy.

## Discussion

Using high-resolution STM imaging and X-ray diffraction, we show that individual **BNPPy** molecules have a remarkable flexibility, which is expressed by the possibility of their pyridyl-terminated substituents to bend in-plane. The terminal pyridyl groups drive the self-assembly, which can be controlled by the choice of the metal substrate. On Ag(111) and Ag(100) surfaces, the molecule-substrate interaction is weak and no influence of the surface was observed. The self-assembly is driven by intermolecular short-range vdW forces and H-bonding leading to a very dense-packed network ( $0.34$  molecules/nm<sup>2</sup>) and no evidence of metal coordination has been observed. Previous studies have been devoted to the coordination chemistry of pyridyl-functionalized molecules in the quest to achieve supramolecular networks.<sup>[20–27]</sup> In particular, utilizing Cu atoms as metallic coordination nodes, two-fold pyridyl-Cu-pyridyl coordination has been reported on Ag(111) and Cu(111).<sup>[19,20,22]</sup> However, a coordinated **BNPPy** network could not be achieved on silver surfaces, neither by annealing nor by providing additional

Cu atoms within the experimental parameter space that was explored.

Contrary to borazine derivatives terminating with phenyl moieties,<sup>[13]</sup> **BNPPy** forms a highly ordered assembly on Cu(111), in which chain-like structures are formed involving Cu coordination. The resulting porous network features a clearly reduced packing density (0.20 molecules/nm<sup>2</sup>) compared to that formed by **BNPPy** on Ag(111) and Ag(100), as well as compared to similar phenyl-terminated borazine derivatives on Cu(111) (0.33 molecules/nm<sup>2</sup>).<sup>[13]</sup> Thus, pyridyl-mediated metal-coordination allows for the fabrication of stable borazine arrays with unprecedented pore sizes. Interestingly, this network does not reflect the three-fold symmetry of **BNPPy**, but bases on interconnected rows where only one of the three py-substituents seems to engage in Cu coordination. Even if we cannot exclude the presence of some coordinative interactions along the rows, our data suggest the simultaneous expression of metal-organic and organic bonding motifs.<sup>[28,29]</sup> The measured center-to-center distance between **BNPPy** units along the coordinated substituents – *i.e.*, perpendicular to the chain direction – is (32.2 ± 0.6) Å. With a py-substituent length of 14.4 Å, extracted from the structural model (after geometry optimization with the semi-empirical AM1 framework in HyperChem<sup>[30]</sup>), this results in a projected pyridyl-Cu-pyridyl bond length of 3.4 Å, slightly reduced compared to the 3.6 Å reported in literature.<sup>[21,24,25,29]</sup> This can be rationalized by the in-plane bending of the substituents. Accordingly, the projected N-Cu bond length corresponds to 1.7 Å. A fully reticulated coordination network with a three-fold symmetry can be achieved by the deposition of additional Cu atoms. This three-fold Cu coordination has been reported only for CN end groups,<sup>[31]</sup> and for bipyridyl molecules.<sup>[32]</sup> Previous studies on molecules with pyridyl-terminated moieties report a favorable two-fold Cu-pyridyl coordination,<sup>[20–25,27,33]</sup> while a rarely observed three-fold coordination motif has been assigned to the presence of Cu dimers in the node expressed as a bright protrusion in STM images.<sup>[21]</sup> As these protrusions are not observed in our assemblies, we speculate that one Cu atom coordinates with the N atoms of three terminal pyridyl groups of the substituents, with typical N-Cu bond distances of (3.0 ± 0.5) Å. This N-Cu bond distance in the three-fold node significantly exceeds the theoretically predicted value of 1.6 Å<sup>[24]</sup> as well as the 1.7 Å characteristic for the two-fold motif, which might reflect the steric hindrance between the (nearly) co-planar pyridyl rings. However, we cannot exclude a minor rotation of the terminal pyridyl moieties out of the surface plane. For instance, such rotations can enable a four-fold coordination of tetra-pyridyl-porphyrins to the mononuclear centers.<sup>[34]</sup>

Our STS data on **BNPPy** and **BNAPy** molecules show that the surface state feature is still detected on the molecular core on both the Cu(111) and the Ag substrates. This observation, together with the XPS data provides evidence that the borazine core is decoupled from the metallic substrates by means of the methyl substituents, a fact which has been anticipated for similar borazine derivatives in a previous report.<sup>[13]</sup> Additionally, the binding energy of the N 1s core level is found to be 399.2 eV, comparable to the ones observed for other borazine derivatives,<sup>[10]</sup> and *h*-BN on metallic substrates.<sup>[35]</sup> The different contributions of the N atoms located in the borazine core and in the pyridyl moieties could not be resolved with our lab-based XPS setup.

## Conclusions

In summary, we combined pyridyl-functionalized borazine derivatives with selected substrates to achieve distinct network architectures, exploiting the remarkable flexibility of the substituents. While the **BNPPy** molecules form a dense-packed hexagonal network on Ag substrates, a porous network evolves for **BNPPy** and **BNAPy** on Cu(111) with stability up to room temperature. The deposition of additional Cu atoms yields a structural transformation of the metal-organic architecture on Cu(111), which leads to an unprecedented fully reticulated network with a three-fold pyridyl-Cu coordination motif. Following this approach, the molecular density could be varied from 0.20 mol/nm<sup>2</sup> to 0.18 mol/nm<sup>2</sup>, expanding the corresponding pore size from 0.7 nm<sup>2</sup> to 6.0 nm<sup>2</sup>. These findings thus provide the first metal-organic coordination architectures on surfaces based on BNC-containing molecules. Our experiments likely suggest that the presence of the sterically shielding methyl groups on the aryl B-bearing substituents prevents the adsorption of CO on the BN core, notwithstanding, they electronically decouple the BN core from the conducting substrate. This findings provide valuable insight for the design of borazine derivatives targeting the anchoring of CO in functional nanostructures comprising for example functionalized hybrid BNC polyphenylenes and graphene-like structures.<sup>[2]</sup>

## Experimental Section

Most STM experiments were carried out in a custom-designed ultra-high vacuum (UHV) chamber housing a CreaTec STM operated at 5 K. Additional STM and XPS experiments were conducted at room temperature in a second UHV chamber equipped with a SPECS X-ray source with an Al anode, a SPECS PHOIBOS 100 electron analyzer and a CreaTec room temperature STM. The base pressure during all experiments was <5×10<sup>-10</sup> mbar. The Cu(111) and the Ag(100) single crystals were prepared by repeated cycles of Ar<sup>+</sup> ion sputtering and annealing to 775 K and 725 K, respectively. Ag(111) films were prepared by e-beam evaporation of several layers of Ag on a Cu(111) crystal, which was held at 575 K as detailed in ref. <sup>[36]</sup>. The borazine derivatives **BNPPy** and **BNAPy** were dosed from a thoroughly degassed quartz crucible held at 600 K onto the sample held at room temperature. All STM images were recorded in constant-current mode using an electrochemically etched tungsten tip. The WSxM software was used to process the STM raw data.<sup>[37]</sup> All XP core-level spectra were excited with the Al K $\alpha$  photon energy 1486 eV. A Shirley-type background was subtracted and Voigt profiles were used to model the data.

## Acknowledgements

This work is supported by the European Research Council Consolidator Grant NanoSurfs (No. 615233) and the Munich-Center for Advanced Photonics (MAP). M.G. would like to acknowledge the H2020-MSCA-IF-2014 programme. W.A. acknowledges funding by the Deutsche Forschungsgemeinschaft *via* a Heisenberg professorship. D.B. thanks the Cardiff University for the financial support.

**Keywords:** borazine derivative • self-assembly • coordination • scanning tunneling microscopy • surface chemistry

[1] D. Bonifazi, F. Fasano, M. M. Lorenzo-Garcia, D. Marinelli, H. Oubaha, J. Tasseroul, *Chem. Commun.* **2015**, 51, 15222.

[2] M. M. Lorenzo-García, D. Bonifazi, *Chimia* **2017**, 71, 550.

- [3] a) I. H. T. Sham, C.-C. Kwok, C.-M. Che, N. Zhu, *Chem. Commun.* **2005**, 1, 3547; b) P. J. Fazen, E. E. Remsen, J. S. Beck, P. J. Carroll, A. R. McGhie, L. G. Sneddon, *Chem. Mater.* **1995**, 7, 1942.
- [4] A. Wakamiya, T. Ide, S. Yamaguchi, *J. Am. Chem. Soc.* **2005**, 127, 14859.
- [5] S. Kervyn, O. Fenwick, F. Di Stasio, Y. S. Shin, J. Wouters, G. Accorsi, S. Osella, D. Beljonne, F. Cacialli, D. Bonifazi, *Chem. - Eur. J.* **2013**, 19, 7771.
- [6] N. A. Riensch, A. Deniz, S. Kühl, L. Müller, A. Adams, A. Pich, H. Helten, *Polym. Chem.* **2017**, 8, 5264.
- [7] a) P. Karamanis, N. Otero, C. Pouchan, *J. Am. Chem. Soc.* **2014**, 136, 7464; b) N. Otero, C. Pouchan, P. Karamanis, *J. Mater. Chem. C* **2017**, 5, 8273; c) N. Otero, P. Karamanis, K. E. El-Kelany, M. Rérat, L. Maschio, B. Civalieri, B. Kirtman, *J. Phys. Chem. C* **2016**, 121, 709.
- [8] a) P. G. Campbell, A. J. V. Marwitz, S.-Y. Liu, *Angew. Chem., Int. Ed. Engl.* **2012**, 51, 6074; b) Z. Liu, T. B. Marder, *Angew. Chem., Int. Ed. Engl.* **2008**, 47, 242; c) X.-Y. Wang, J.-Y. Wang, J. Pei, *Chem. - Eur. J.* **2015**, 21, 3528; d) H. Helten, *Chem. - Eur. J.* **2016**, 22, 12972.
- [9] X. Wang, G. Sun, P. Routh, D.-H. Kim, W. Huang, P. Chen, *Chem. Soc. Rev.* **2014**, 43, 7067.
- [10] F. Ciccullo, A. Calzolari, I. P. S.-A. Savu, M. Krieg, H. F. Bettinger, E. Magnano, T. Chassé, M. B. Casu, *J. Phys. Chem. C* **2016**, 120, 17645.
- [11] a) K. T. Jackson, M. G. Rabbani, T. E. Reich, H. M. El-Kaderi, *Polym. Chem.* **2011**, 2, 2775; b) T. E. Reich, S. Behera, K. T. Jackson, P. Jena, H. M. El-Kaderi, *J. Mater. Chem.* **2012**, 22, 13524.
- [12] a) F. Rosei, M. Schunack, Y. Naitoh, P. Jiang, A. Gourdon, E. Laegsgaard, I. Stensgaard, C. Joachim, F. Besenbacher, *Prog. Surf. Sci.* **2003**, 71, 95; b) L. Piot, C. Marie, X. Feng, K. Müllen, D. Fichou, *Adv. Mater.* **2008**, 20, 3854; c) S. Schlögl, T. Sirtl, J. Eichhorn, W. M. Heckl, M. Lackinger, *Chem. Commun.* **2011**, 47, 12355; d) B. Cirera, J. Matarrubia, T. Kaposi, N. Giménez-Agulló, M. Paszkiewicz, F. Klappenberger, R. Otero, J. M. Gallego, P. Ballester, J. V. Barth, R. Miranda, J. R. Galán-Mascarós, W. Auwärter, D. Écija, *Phys. Chem. Chem. Phys.* **2017**, 19, 8282.
- [13] N. Kalashnyk, P. Ganesh Nagaswaran, S. Kervyn, M. Riello, B. Moreton, T. S. Jones, A. de Vita, D. Bonifazi, G. Costantini, *Chem. - Eur. J.* **2014**, 20, 11856.
- [14] a) J. I. Urgel, M. Schwarz, M. Garnica, D. Stassen, D. Bonifazi, D. Écija, J. V. Barth, W. Auwärter, *J. Am. Chem. Soc.* **2015**, 137, 2420; b) J. V. Barth, *Surf. Sci.* **2009**, 603, 1533; c) K. Ariga, V. Malgras, Q. Ji, M. B. Zakaria, Y. Yamauchi, *Coord. Chem. Rev.* **2016**, 320-321, 139; d) L. Dong, Z. A. Gao, N. Lin, *Prog. Surf. Sci.* **2016**, 91, 101.
- [15] D. Écija, S. Vijayaraghavan, W. Auwärter, S. Joshi, K. Seufert, C. Aurisicchio, D. Bonifazi, J. V. Barth, *ACS Nano* **2012**, 6, 4258.
- [16] C. Sánchez-Sánchez, S. Brüller, H. Sachdev, K. Mullen, M. Krieg, H. F. Bettinger, A. Nicolai, V. Meunier, L. Talirz, R. Fasel, P. Ruffieux, *ACS Nano* **2015**, 9, 9228.
- [17] J. Zirot, P. Gold, A. Bendounan, F. Forster, F. Reinert, *Surf. Sci.* **2009**, 603, 354.
- [18] Z. Yang, M. Corso, R. Robles, C. Lotze, R. Fitzner, E. Mena-Osteritz, P. Bäuerle, K. J. Franke, J. I. Pascual, *ACS Nano* **2014**, 8, 10715.
- [19] T. R. Umbach, M. Bernien, C. F. Hermanns, L. L. Sun, H. Mohrmann, K. E. Hermann, A. Krüger, N. Krane, Z. Yang, F. Nickel, Y.-M. Chang, K. J. Franke, J. I. Pascual, W. Kuch, *Phys. Rev. B* **2014**, 89, 235409.
- [20] F. Klappenberger, A. Weber-Bargioni, W. Auwärter, M. Marschall, A. Schiffrin, J. V. Barth, *J. Chem. Phys.* **2008**, 129, 214702.
- [21] D. Heim, D. Écija, K. Seufert, W. Auwärter, C. Aurisicchio, C. Fabbro, D. Bonifazi, J. V. Barth, *J. Am. Chem. Soc.* **2010**, 132, 6783.
- [22] D. Heim, K. Seufert, W. Auwärter, C. Aurisicchio, C. Fabbro, D. Bonifazi, J. V. Barth, *Nano Lett.* **2010**, 10, 122.
- [23] A. Langner, S. L. Tait, N. Lin, R. Chandrasekar, M. Ruben, K. Kern, *Angew. Chem., Int. Ed. Engl.* **2008**, 47, 8835.
- [24] Y. Li, J. Xiao, T. E. Shubina, M. Chen, Z. Shi, M. Schmid, H.-P. Steinrück, J. M. Gottfried, N. Lin, *J. Am. Chem. Soc.* **2012**, 134, 6401.
- [25] S. L. Tait, A. Langner, N. Lin, S. Stepanow, C. Rajadurai, M. Ruben, K. Kern, *J. Phys. Chem. C* **2007**, 111, 10982.
- [26] F. Studener, K. Müller, N. Marets, V. Bulach, M. W. Hosseini, M. Stohr, *J. Chem. Phys.* **2015**, 142, 101926.
- [27] T. Lin, X. S. Shang, J. Adisojojoso, P. N. Liu, N. Lin, *J. Am. Chem. Soc.* **2013**, 135, 3576.
- [28] S. Vijayaraghavan, D. Écija, W. Auwärter, S. Joshi, K. Seufert, M. Drach, D. Nieckarz, P. Szabelski, C. Aurisicchio, D. Bonifazi, J. V. Barth, *Chem. - Eur. J.* **2013**, 19, 14143.
- [29] F. Bischoff, Y. He, K. Seufert, D. Stassen, D. Bonifazi, J. V. Barth, W. Auwärter, *Chem. - Eur. J.* **2016**, 22, 15298.
- [30] HyperChem, Hypercube Inc., 1115 NW St., 32601, Gainesville, FL, U.S.A., www.hyper.com.
- [31] a) G. E. Pacchioni, M. Pivetta, H. Brune, *J. Phys. Chem. C* **2015**, 119, 25442; b) T. Sirtl, S. Schlögl, A. Rastgoo-Lahrood, J. Jelic, S. Neogi, M. Schmittel, W. M. Heckl, K. Reuter, M. Lackinger, *J. Am. Chem. Soc.* **2013**, 135, 691; c) G. Pawin, K. L. Wong, D. Kim, D. Sun, L. Bartels, S. Hong, T. S. Rahman, R. Carp, M. Marsella, *Angew. Chem., Int. Ed. Engl.* **2008**, 47, 8442.
- [32] a) A. Langner, S. L. Tait, N. Lin, R. Chandrasekar, V. Meded, K. Fink, M. Ruben, K. Kern, *Angew. Chem., Int. Ed. Engl.* **2012**, 51, 4327; b) S. L. Tait, A. Langner, N. Lin, R. Chandrasekar, O. Fuhr, M. Ruben, K. Kern, *ChemPhysChem* **2008**, 9, 2495.
- [33] a) Y. Li, N. Lin, *Phys. Rev. B* **2011**, 84, 125418; b) Z. Shi, N. Lin, *J. Am. Chem. Soc.* **2009**, 131, 5376.
- [34] B. Wurster, D. Grumelli, D. Hötger, R. Gutzler, K. Kern, *J. Am. Chem. Soc.* **2016**, 138, 3623.
- [35] A. B. Preobrajenski, A. S. Vinogradov, N. Mårtensson, *Surf. Sci.* **2005**, 582, 21.
- [36] M. Garnica, M. Schwarz, J. Ducke, Y. He, F. Bischoff, J. V. Barth, W. Auwärter, D. Stradi, *Phys. Rev. B* **2016**, 94, 155431.
- [37] I. Horcas, R. Fernández, J. M. Gómez-Rodríguez, J. Colchero, J. Gómez-Herrero, A. M. Baro, *Rev. Sci. Instrum.* **2007**, 78, 013705-1 - 013705-8.

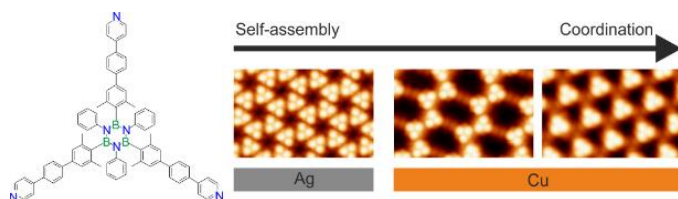


---

Layout 2:

## FULL PAPER

---



**Borazine Derivatives on coinage metals:** The network structure of decoupled borazine derivatives can be tuned by the employed noble metal substrate. On Ag(111) films, a dense-packed self-assembly is observed, while on Cu(111) a porous architecture can be transformed into a fully coordinated metal-organic network by exposure to additional metal adatoms.

*Martin Schwarz, Manuela Garnica,  
Francesco Fasano Nicola Demitri,  
Davide Bonifazi,\* and Willi Auwärter\**

**Page No. – Page No.**

**BN-Patterning of Metallic Substrates  
through Metal Coordination of  
Decoupled Borazines**

---